# Expanding Grassland Coverage Maintain Ecohydrological Sustainability in the Agro-Pastoral Ecotone of Northwest China

Yuzuo Zhu[1], Xuefeng Xu[1]

[1] Key Laboratory of West China's Environmental System (Ministry of Education), College of Earth and Environmental Sciences, Lanzhou University, Lanzhou, Gansu 730000, China

*Correspondence to*: Yuzuo Zhu (zhuyz16@lzu.edu.cn)

**Abstract.** To achieve ecological sustainability, the Chinese government is conducting large-scale vegetation restoration projects to increase grasslands to 60 % by 2035. However, excessive vegetation restoration undermined soil drying in the agro-pastoral ecotone of Northwest China (APENWC), where grasslands made up 52.0%, barren land 29.9%, and croplands 12.5% in 2015, with other classes accounting for 5.6%. It is unclear the potential impacts of future land use/cover change (LUCC) on ecohydrological sustainability over the APENWC. To address this gap, the Community Land Model (version 5.0, CLM5.0) was implemented for the historical period 2000–2015 under a real LUCC scenario (reference scenario) and several synthetic LUCC scenarios. The impacts of the LUCC on regional water fluxes and temperature were assessed by comparing the spatially averaged annual land surface temperature (LST) and evapotranspiration (ET) simulated using different model setups. The reference scenario revealed two main LUCC types in the region: conversions from bare land to grasslands and from croplands to grasslands, with a total increase in grassland cover from 44.8 % in 2000 to 52.0 % in 2015. The conversion from bare land to grasslands reduced LST by 0.17 °C and increased ET by 53.32 mm yr$^{-1}$. Conversely, the conversion from croplands to grasslands increased LST by 1.18 °C and reduced ET by 190.89 mm yr$^{-1}$. Despite these significant local LUCC impacts, the overall effect of the historical LUCC resulted in limited variations in LST (-0.06 °C) and ET (9.70 mm yr$^{-1}$) when the complete APENWC region is considered. Future scenarios assuming 60 % grassland cover with varying proportions of bare land and cropland suggest that none of the scenarios showed significant adverse effects on WC, suggesting that vegetation restoration will not intensify drying conditions. These results indicate that increasing grassland coverage to 60% by 2035 supports ecohydrological sustainability without introducing drying.

**Keywords**: Land use/cover change, Water conservation, CLM5.0, Land use composition, Agricultural-pastoral ecotone in Northwest

## 1 Introduction

Land use/cover change (LUCC), including deforestation, afforestation, grassland restoration, and agricultural expansion, profoundly affects energy and vapour interactions at the land-atmosphere interface (Alkama and Cescatti, 2016; Woodward et al., 2014; Duveiller et al., 2018). These changes alter biogeophysical characteristics, thereby influencing climate and hydrology

30   on regional and global scales (Chen and Dirmeyer, 2016; Davin et al., 2020; Liu et al., 2016). LUCC has been recognised as a key mitigation and adaptation strategy for climate and hydrological challenges, particularly under global warming and water resource constraints (Arora and Montenegro, 2011; Davin et al., 2014; Findell et al., 2017; Poniatowski et al., 2020). Understanding the impacts of LUCC and integrating these insights into policymaking processes is essential to promote sustainable land management practices and enhance ecosystem services (Jia et al., 2017a; Zhang et al., 2018).

35   To examine the effects of LUCC, researchers have employed statistical analyses based on in-situ observations, satellite products, and numerical models (Lee et al., 2011; Nkhoma et al., 2021). However, in-situ observations are often sparsely and unevenly distributed owing to equipment and resource limitations (Li et al., 2021; Zhang et al., 2021), while satellite products frequently lack accurate, continuous long-term data because of instantaneous image acquisition and uncertainties introduced by processing methods (Srivastava et al., 2015; Zhang et al., 2010). However, numerical models enable the investigation of

40   multiple variables with high spatial resolution over extended periods, offering a consistent framework for analysing flux cycles (Han et al., 2021; Winckler et al., 2018). Numerous studies have used numerical models to systematically interpret water and energy processes, thereby significantly our advancing the understanding of LUCC impacts (Chen and Dirmeyer, 2019; Llopart et al., 2018). The Community Land Model (CLM), in which each grid cell is composed of multiple land use/cover classes, effectively simulates changes in water and energy processes in response to LUCC across different regions (Li, 2021; Meier et

45   al., 2018; Xu et al., 2020; Lawrence et al., 2019).

  Land surface temperature (LST) and evapotranspiration (ET) are highly sensitive to the LUCC and are critical indicators for evaluating extreme events and managing water resources (Chen and Dirmeyer, 2018; He et al., 2020; Li et al., 2015; Wang et al., 2020). The effects of the LUCC on LST vary primarily because of competition among different biogeophysical characteristics, such as surface albedo, surface roughness, and evapotranspiration (Burakowski et al., 2018; Cherubini et al.,

50   2018; Davin and De Noblet-Ducoudré, 2010; Li et al., 2015). Similarly, the LUCC affects ET by altering the redistribution of moisture fluxes and energy balance, which differs according to the LUCC type and spatial variability (Das et al., 2018; Li et al., 2017; Ning et al., 2017; Winckler et al., 2017). The diurnal cycle is often employed to reveal discrepancies in flux distribution, such as soil residual heat flux and latent heat flux, and to illustrate how biogeophysical characteristics during the LUCC influence energy and water cycles (Breil et al., 2020; Kueppers and Snyder, 2011). Despite extensive research

55   quantifying the spatially averaged impacts of LUCC and the individual effects of specific LUCC types on LST and ET (Cherubini et al., 2018; Davin and De Noblet-Ducoudré, 2010), few studies have attributed these effects to the synergistic effects of multiple LUCC types under realistic and complex conditions. Therefore, LST and ET were chosen as representative variables to quantify the individual and spatially averaged impacts of different LUCC types and to analyse how the combination of LUCC impacts resulted in unclear or mixed synergistic effects.

60   The agro-pastoral ecotone of Northwest China (APENWC) is characterized by an interlaced mosaic of grasslands, croplands, and bare land (Li et al., 2018; Xue et al., 2019; Yang et al., 2021a). Since the 1980s, policies such as the "Grain for Green Project" and the "Three-North Shelterbelt" have led to substantial changes in land surface vegetation, increasing vegetation coverage and restoring degraded areas (Cao et al., 2015; Wei et al., 2018; Liu et al., 2019). These initiatives have enhanced

vegetation growth (Wang et al., 2019b; Wu et al., 2013; Xue et al., 2019; Zhang et al., 2018) and resulted in reduced runoff

65  (Liang et al., 2015; Zhang et al., 2016), increased ET (Wang et al., 2019a), and decreased LST (Wang et al., 2020). However, excessive vegetation restoration has been reported to undermine ecohydrological sustainability, leading to challenges such as soil drying (Jia et al., 2017b; Zhang et al., 2018). These findings highlight the urgent need for land use/cover configurations that balance vegetation restoration with ecohydrological sustainability in the APENWC. Additionally, the latest national ecological development plan, implemented from 2021 to 2035, aims to increase grassland coverage to 60 % and convert bare

70  land and croplands into grasslands to enhance ecosystem services ((China state council, 2017; National developmen tand reform commission, 2019). However, this ambitious target has not been thoroughly assessed for its potential impacts on ecohydrological sustainability.

Previous research has optimised land use/cover configurations based on a multi-objective genetic algorithm integrating economic and ecological parameters (Kaim et al., 2018; Kucsicsa et al., 2019; Yang et al., 2020). However, these experimental

75  designs were constrained by limited theoretical exploration of parameter settings (Ding et al., 2021) and could not meet the government's predefined targets, such as achieving 60 % grassland coverage. This study examined the impacts of historical and future LUCC associated with vegetation restoration projects in APENWC using the Community Land Model (version 5.0, CLM5.0). Section 2 provided an overview of the CLM5.0 framework and details the experimental design. Section 3.1 analysed the spatially averaged impacts of LUCC during the historical period of 2000–2015 under a realistic LUCC scenario.

80  Additionally, the individual impacts of different LUCC types were quantified using idealised scenarios where specific LUCC types are maximised. Section 3.2.1 categorized the historical land use/cover composition from 2000 to 2015 and attributed the spatially averaged impacts to the synergistic effects of multiple LUCC types. Finally, Section 3.2.2 introduced future LUCC scenarios designed to achieve the government's target of 60 % grassland coverage. These scenarios were evaluated to assess their potential effects on water conservation (WC) in the APENWC. Section 4 discussed the experimental results, while Section

85  5 summarised the study's key findings.

## 2 Materials and Methods

### 2.1 Study area

The boundaries of agro-pastoral ecotone are not universally defined, as they vary depending on ecological, climatological, and economic geographic indicators (Li et al., 2021). The APENWC was delineated based on previous research (Wang et al., 2020;

90  Tan et al., 2020) and includes Otog Banner, Otog Front Banner, Lingwu, Yanchi, Dingbian, Jingbian, Hengshan, Yuyang, Wushen, and Shenmu. It is situated in the northwestern part of the agro-pastoral ecotone of Northern China (APENC). It spans from 36.816 to 40.194 °N and 106.228 to 110.903 °E (Fig. 1). The region covers an area of 77,513 km², with elevations ranging from 915 to 1,947 m above sea level. The area experiences an average annual temperature between 7.0 and 9.0 °C, average relative humidity of 13 %, and annual precipitation of 250 to 450 mm, with most rainfall occurring in the summer (Xu et al.,

95  2020; Yang et al., 2021a). The dominant land use/cover classes in the sequence were grasslands, bare land, and croplands. The

APENWC serves as a climatic and ecological transitional zone historically shaped by agricultural cultivation and animal husbandry. It is susceptible to changes in human activities and background climatic conditions (Tan et al., 2020; Wei et al., 2018; Xue et al., 2019).
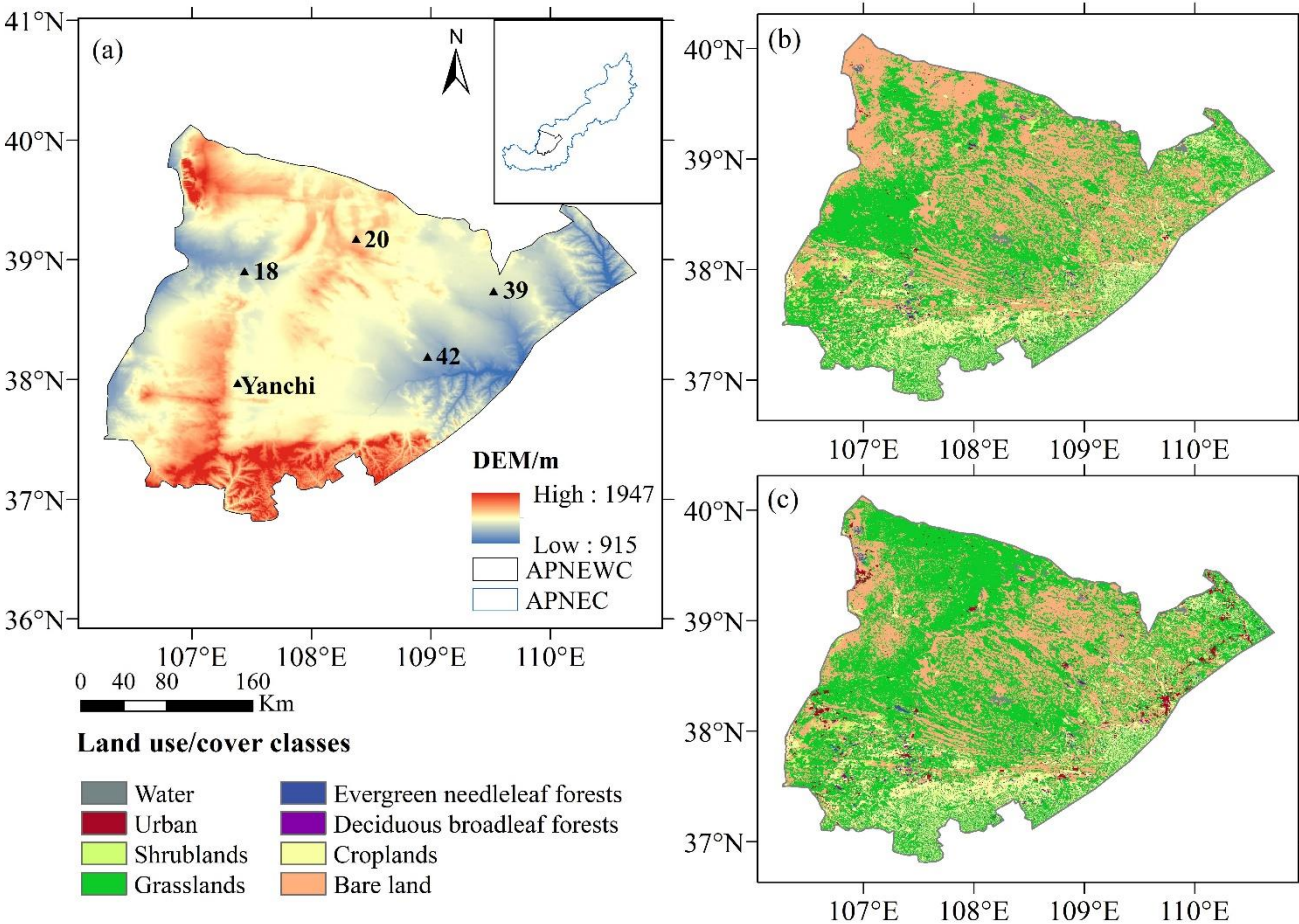
**Figure 1. (a) DEM of the APNEWC region showing the locations of in-situ observation stations. Land use/cover map of the study area in 2000 (b) and 2015 (c).**

## 2.2 Datasets

The surface land use/cover dataset, with a resolution of 30 m × 30 m, was utilised to analyse the land use/cover in 2000 and 2015, representing the pre- and post-vegetation restoration conditions. It classifies eight land use/cover classes: shrublands, grasslands, croplands, urban areas, barren land, water bodies, evergreen needleleaf forests, and deciduous broadleaf forests, consistent with the CLM5.0 input requirements. Rainfed and irrigated croplands data were calculated using the ratio of irrigated land to cultivated land in the Shanxi, Ningxia, and Erdos Yearbooks. The percentage of rainfed and irrigated croplands on the APENWC was 61.30 and 38.70 in 2000, and 46.48 and 53.52 in 2015, respectively (Xu, 2018; Yang, 2021). Meteorological inputs were obtained from the China Meteorological Forcing Dataset (CMFD, http://data.tpdc.ac.cn), which provides a 3 h

110 temporal resolution and 0.1 ° spatial resolution spanning the year from 1979 to 2018 (Yang and He, 2016). Soil properties, including sand, clay, organic matter, and bulk density, were obtained from the soil properties dataset for land surface modelling over China (http://data.tpdc.ac.cn) with a $30 \times 30$ arcsec resolution  (Shangguan and Dai, 2013).

To validate the model outputs, six in-situ observation stations (Table S1) were established in 2016. Two stations located in Yanchi were designated for croplands and grasslands, three additional stations (Sites 18, 20, and 39) were focused on
115 grasslands, and Site 42 was dedicated to croplands. Soil temperature and moisture were monitored at half-hour intervals starting in August 2016 using ECH20 sensors that  recorded data from the soil layers at depths of 0–5 cm, 5–10 cm, 10–15 cm, 15–30 cm, and 30–50 cm. MODIS LST (https://lpdaac.usgs.gov/dataset_discovery/modis) with 0.05 ° spatial resolution was used to validate LST (Wan et al., 2015). ET and net radiation were validated over the domain using two sensing products from GLASS (http://glass-product.bnu.edu.cn/). ET with 8-day temporal resolution and 0.05 ° spatial resolution and surface all-wave daily
120 net radiation with daily temporal resolution and 0.05 ° spatial resolution (Guo et al., 2020; Yao et al., 2014).

All datasets (Table S2) were interpolated to 0.1 ° grids to match the model outputs. The surface land use/cover dataset covering the study area was evaluated in a previous study, and its precision was reliable (Du et al., 2020). The China meteorological forcing dataset and MODIS LST have been widely used in the study area (Li, 2021; Wang et al., 2020). Other datasets were evaluated in the papers that produced the data. The uncertainty in the soil properties is discussed in Section 4.2.

125 **2.3 Model description**

CLM5.0, developed by the National Center for Atmospheric Research (NCAR) as the land surface component of the Community Earth System Model (CESM, http://www.cesm.ucar.edu/models/cesm2/), is a land surface model that includes biogeophysical and biogeochemical processes (Lawrence et al., 2019). Each grid cell in CLM5.0 includes multiple land units, such as vegetated areas, crops, lakes, urban areas, and glaciers. The vegetated land unit is divided into 16 plant functional types
130 (PFTs) in the SP (Satellite Phenology) compset (Bonan et al., 2002; Lawrence et al., 2019). Details of the latest CLM5.0 can be found in the technical description in version 5.0 (http://www.cesm.ucar.edu/models/cesm2/land/CLM50_Tech_Note.pdf). To represent local crops in the APENWC, we modified the parameters for the C3 unmanaged crop in the SP compset and classified it as corn. These modifications included assigning a leaf area index (LAI) of 0 for the non-growing season, a vegetation height of 1.65 m based on field measurements (2017–2018), and a stem area index (SAI) of 0.1* LAI.

135 The domain was implemented in CLM5.0 with $40 \times 50$ grid cells and a spacing of 0.1 °. Each grid cell contains multiple land use/cover classes. The spin-up time to reach equilibrium was constrained by $|Var_{n+1}-Var_n| < 0.001*|Var_n|$ (Cai et al., 2014; Yang et al., 1995), where 'Var' represents each variable and 'n' is the spin-up year. The soil moisture was selected as the constrained variable (Fig. S1) according to Han et al. (2021). The atmospheric forcing from 1979 to 2018 was cycled twice to run the spin-up. Thus, the results for 2000 and 2015 reached an equilibrium and were used in the analysis. The model outputs
140 were configured with a temporal resolution of 3 h.

## 2.4 LUCC experimental design

Table 1 provides the details of the experiments conducted. Single-point simulations with maximised single land use/cover class were compared with in-situ observations to assess CLM5.0 performance under different land use/cover conditions. CN2000 and CN2015 simulated the actual land use/cover and atmospheric forcing to evaluate the accuracy of the model over
145    the entire domain.

A suite of land use/cover scenario experiments was designed to explore the impacts of the LUCC. The only difference between the land use/cover scenario experiments was the land use/cover, which ensured that the impacts of the LUCC were isolated. The impact of LUCC from 2000 to 2015 was quantified by comparing EXP2000 and CN2015 (Wang et al., 2020; Breil et al., 2020). Three additional experiments examined the effect of individual LUCC: EXP_bare and EXP_crop scenarios, respectively,
150    extended bare land and croplands to 100 %, whereas EXP_grass set grasslands to 100 %, replacing bare land and croplands (Cherubini et al., 2018). To evaluate vegetation restoration in the APENWC, future land use/cover scenarios were conducted by setting the percentage of grasslands at 60 % and varying proportions of croplands and bare land simulated in EXP_602113, EXP_602311, EXP_602509, EXP_602707, and EXP_603004.

Finally, additional sensitivity simulations were conducted in which specific biogeophysical parameters were altered while
155    other settings remained the same as those in the Yanchi_grass simulation. In the Yanchi_laisai simulation, the leaf and stem area index (LAI + SAI) of grasslands was replaced by LAI + SAI of cropland. Similarly, in the Yanchi_height simulation, the vegetation height of grasslands was substituted with the vegetation height of cropland (Breil et al., 2020). These sensitivity experiments aimed to explore the influence of biogeophysical factors in regulating energy and vapour fluxes during LUCC.

**Table 1. List of numerical simulations.**

| Experiment | Region/points | Land use/cover | Atmospheric Forcing | Grid |
|---|---|---|---|---|
| Yanchi_grass | Yanchi | Grasslands | 2015–2018 | 0.0001 ° |
| Yanchi_crop | Yanchi | Croplands | 2015–2018 | 0.0001 ° |
| 18_grass | 18 | Grasslands | 2015–2018 | 0.0001 ° |
| 20_grass | 20 | Grasslands | 2015–2018 | 0.0001 ° |
| 39_grass | 39 | Grasslands | 2015–2018 | 0.0001 ° |
| 42_crop | 42 | Croplands | 2015–2018 | 0.0001 ° |
| CN2000 | Domain | 2000 | 2000 | 0.1 ° |
| CN2015 | Domain | 2015 | 2015 | 0.1 ° |
| EXP2000 | Domain | 2000 | 2015 | 0.1 ° |
| EXP_grass | Domain | Grasslands | 2015 | 0.1 ° |
| EXP_bare | Domain | Bare land | 2015 | 0.1 ° |
| EXP_crop | Domain | Croplands | 2015 | 0.1 ° |
| EXP_602113 | Domain | Grasslands 60 %, bare land 21 %, croplands 13 % | 2000–2015 | 0.1 ° |
| EXP_602311 | Domain | Grasslands 60 %, bare land 23 %, croplands 11 % | 2000–2015 | 0.1 ° |
| EXP_602509 | Domain | Grasslands 60 %, bare land 25 %, croplands 9 % | 2000–2015 | 0.1 ° |
| EXP_602707 | Domain | Grasslands 60 %, bare land 27 %, croplands 7 % | 2000–2015 | 0.1 ° |
| EXP_603004 | Domain | Grasslands 60 %, bare land 30 %, croplands 4 % | 2000–2015 | 0.1 ° |
| Yanchi_laisai | Yanchi | Yanchi | 2015 | 0.0001 ° |
| Yanchi_height | Yanchi | Yanchi | 2015 | 0.0001 ° |

160

165

170

**2.5 Criteria of appropriate land use/cover composition**

Considering the importance of warming impacts and the WC function, LST and WC have been introduced as criteria for optimising ecosystem services from the perspective of energy and hydrological cycles (Bai et al., 2019; Zeng and Li, 2019; Wang et al., 2021c). WC was obtained from the water balance using Eq. (1):

175
$$WC = P - ET - Runoff \tag{1}$$

where *WC* is annual water conservation (mm yr$^{-1}$). *P, ET,* and *Runoff* are the annual precipitation (mm yr$^{-1}$), evapotranspiration (mm yr$^{-1}$), and runoff (mm yr$^{-1}$), respectively. P is the forcing data of CLM5.0, and the other data are the outputs of CLM5.0. The model's performance was validated by Li (2021) and described in the next section.

**2.6 Model evaluation**

180   Previous studies have validated the soil moisture output for grasslands and croplands in the APENWC against in-situ observations, demonstrating a high agreement (Li, 2021). The simulated soil temperature in grasslands and croplands also showed a strong correlation with the in-situ observations (Fig. S2), with correlation coefficients (R) of 0.98 (Yanchi grass), 0.98 (Yanchi crop), 0.99 (Site 18), 0.96 (Site 20), 0.97 (Site 39), and 0.96 (Site 42). These sites' BIAS (absolute error) values ranged from -1.24 to 0.09 °C, while the RMSE (root mean squared error) ranged from 2.07 to 3.28 °C. All single-point

185   simulations at five depths exhibited high R (>0.95), low BIAS ($< \pm 1.71$ °C), and low RMSE (<3.88 °C). ET simulations at the Yanchi station also performed well, with R, BIAS, and RMSE values of 0.93, 15.52 mm month$^{-1}$, and 17.10 mm month$^{-1}$, respectively (Fig. S3). Spatiotemporal validation for the entire domain, using MODIS and GLASS datasets, showed R values of 0.96 for LST, 0.84 for net radiation, and 0.83 for ET (Fig. S4). Although parameterisation introduces minimal bias in the performance of CLM5.0 (Deng et al., 2020; Luo et al., 2020; Ma et al., 2021), the effects of LUCC suppress model uncertainty

190   due to parameterisation (Tölle et al., 2018). Thus, CLM5.0 effectively captures the complex and realistic LUCC dynamics in the APENWC.

**3 Results**

**3.1 LUCC**

**3.1.1 Impacts of LUCC from 2000 to 2015**

195   To quantify the spatially averaged and individual impacts of different LUCC types, historical LUCCs from 2000 to 2015 were analysed. During this period, grasslands, forests, and shrublands increased by 7.2 %, 0.3 %, and 0.1 %, respectively, whereas bare land and croplands decreased by 8.7 % and 0.2 %, respectively. Overall, vegetation coverage in the APENWC has increased. The primary LUCC transitions included bare land to grasslands (11.6 %), croplands to grasslands (1.2 %), grasslands to bare land (3.8 %), and grasslands to croplands (1.0 %). The conversion of bare land and croplands to grasslands is largely

200   driven by vegetation restoration projects. Spatially, the conversion from bare land to grasslands was concentrated in the

northewestern APENWC, with scattered occurrences elsewhere, whereas the conversion from grasslands to bare land was predominantly in the western APENWC. The conversion from croplands to grasslands was primarily located in the southwestern APENWC, whereas the conversion from grasslands to croplands was concentrated in the mid-southern APENWC.

205 Figure 2 illustrates the spatial and seasonal temperature differences between CN2015 and EXP2000. From 2000 to 2015, LUCC generally resulted in a cooling effect across large areas of the APENWC, with a spatially averaged cooling of -0.06 ℃, attributed to increased vegetation coverage. The cooling effect was weaker in the eastern APENWC due to the minimal LUCC in this region. Seasonal temperature changes were as follows: -0.06 ℃ in spring (MAM: March, April, and May), -0.12 ℃ in summer (JJA: June, July, and August), -0.06 ℃ in autumn (SON: September, October, and November) and -0.02 ℃ in winter
210 (DJF: December, January, and February).

From 2000 to 2015, LUCC led to an overall increase in ET across the APENWC (Fig. 3), with a mean difference of 9.70 mm yr$^{-1}$ due to enhanced vegetation coverage. Seasonally changes in ET were 1.93 mm in spring, 6.53 mm in summer, 1.16 mm in autumn, and 0.07 mm in winter. The impact of the LUCC on ET was most pronounced during the summer, with weak changes in autumn and winter.

215
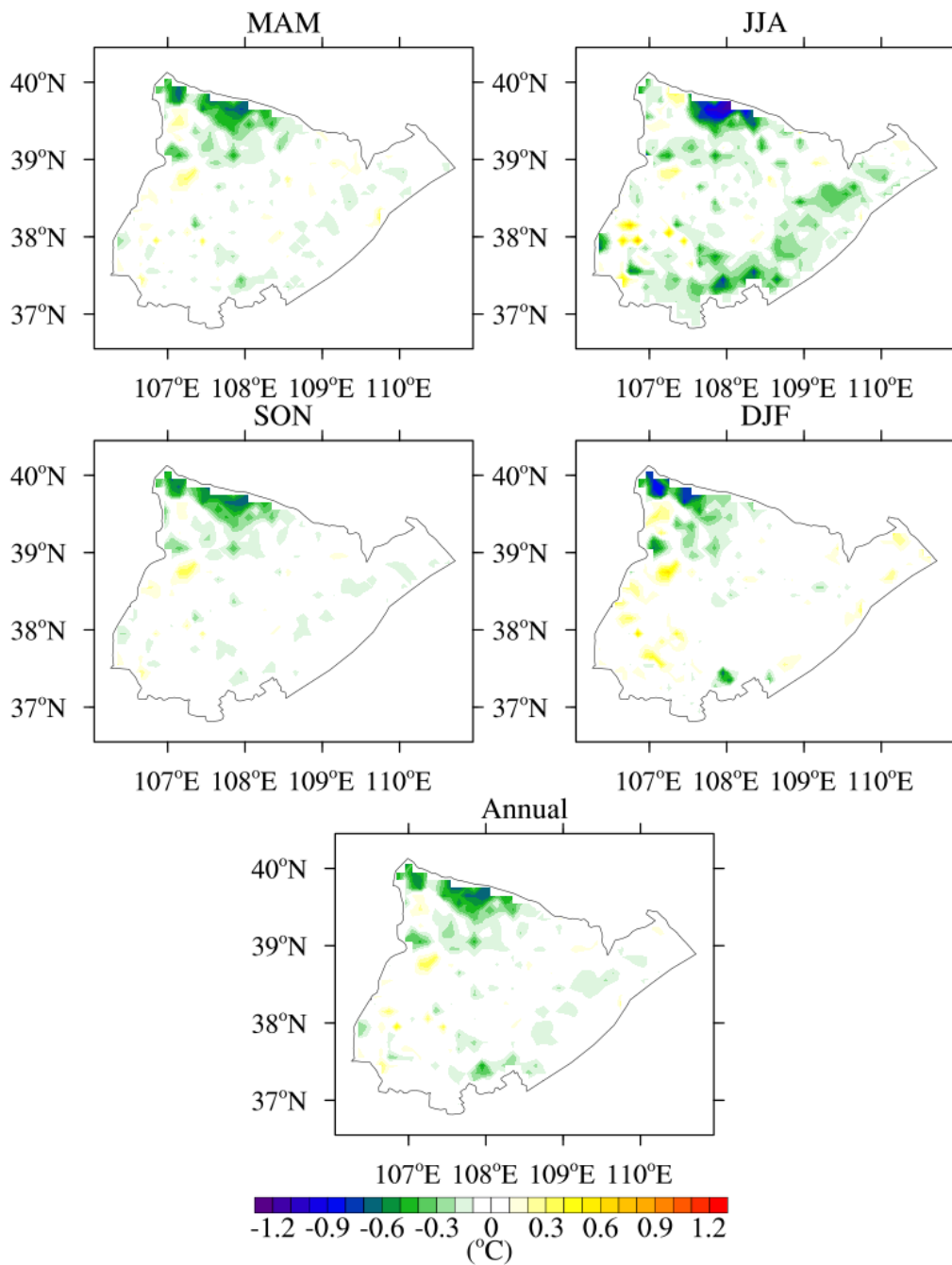
**Figure 2. Differences in spatially averaged land surface temperature (LST) between simulations using 2000 and 2015 land use/cover data (CN2015 - EXP2000).**
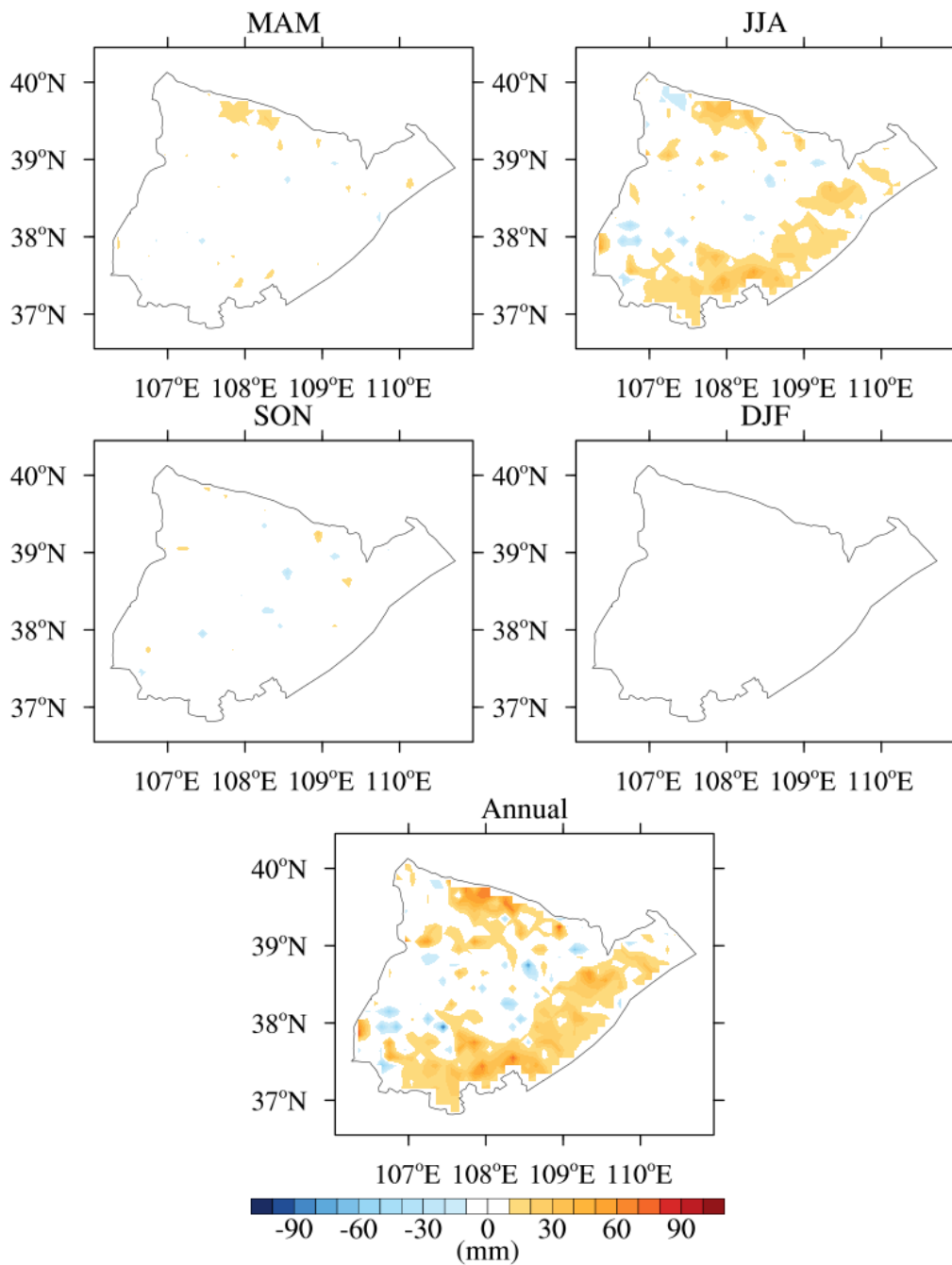
**Figure 3. Differences in spatially averaged evapotranspiration (ET) between simulations using 2000 and 2015 land use/cover data (CN2015 - EXP2000).**

### 3.1.2 Effects of different LUCC types

Different types of LUCC generate distinct impacts, resulting in spatially averaged effects across domains. This analysis focused on the dominant LUCC types: bare land to grasslands, grasslands to bare land, croplands to grasslands, and grasslands to croplands. Grid cells with single LUCC changes (≥15 %) and minor changes in other types (≤15 %) were selected for further investigation (Fig. S5) (Winckler et al., 2018). To examine these effects, two idealised scenarios were designed to represent the primary vegetation restoration types: converting bare land to grasslands and converting croplands to grasslands. One scenario maximised the conversion of bare land to grasslands, and the other maximised the conversion of croplands to grasslands (Arora and Montenegro, 2011; Cherubini et al., 2018). Detailed descriptions of these scenarios are presented in Table 1. Analyses of water and energy process responses to bare land and grassland transitions were conducted in grid cells characterised by intense bare land to grasslands and grasslands to bare land changes (143 grids, Fig. S5). Similarly, analyses of the croplands and grasslands transitions were performed in grid cells with significant croplands to grasslands and grasslands to croplands changes (10 grids, Fig. S5), in which the crops and grass were converted.

The contrasting effects of the two vegetation restoration types are shown in Figure S6. Conversion from bare land to grasslands resulted in an annual average LST reduction of 0.17 °C, whereas conversion from croplands to grasslands led to an annual average LST increase of 1.18 °C. Seasonally, bare land to grasslands conversion caused average cooling effects of -0.15 °C in spring, -0.74 °C in summer, and -0.66 °C in autumn, but a warming effect of 0.89 °C in winter. Conversely, croplands to grasslands exhibited warming effects with a seasonal variation: average LST differences of 0.80 °C in spring, 2.31 °C in summer, 0.47 °C in autumn, and 1.15 °C in winter. Annual changes in ET were 53.32 mm yr$^{-1}$ and -190.89 mm yr$^{-1}$ from the bare land and croplands to grasslands transitions, respectively. Seasonal ET differences for the bare land to grasslands transitions were 15.67 mm season$^{-1}$, 23.28 mm season$^{-1}$, 11.99 mm season$^{-1}$, and 2.37 mm season$^{-1}$ in spring, summer, autumn, and winter, respectively. In contrast, croplands to grasslands showed ET differences of -35.22 mm season$^{-1}$, -134.35 mm season$^{-1}$, -24.19 mm season$^{-1}$, and 2.87 mm season$^{-1}$ in spring, summer, autumn, and winter, respectively.

Further analysis examined the contrasting mechanisms driving the responses of bare land and croplands to grasslands. Complete diurnal cycles were analysed for summer and winter, the two most representative seasons.

#### a. Bare land to grasslands

In the summer of CLM5.0 simulations, LST exhibited cooling from bare land to grasslands (-0.74 °C, Fig. S7). For bare land, the surface temperature is equal to the ground temperature, whereas for vegetated areas. It is influenced by both the ground and vegetation temperatures (Lawrence et al., 2019). The ground temperature is determined by the amount of energy used to warm the ground and soil, residual heat energy. It results from the competition between the net radiative energy input and the sum of the turbulent heat fluxes (sensible and latent heat fluxes) (Breil et al., 2020). As shown in Fig. S7, the differences in ground temperature between bare land and grasslands were minimal (-0.05 °C), indicating that the reduced surface temperature for grasslands was mainly driven by the lower vegetation temperature.

In winter, LST increased by 0.89 °C from bare land to grasslands. The increases in sensible heat flux and latent heat flux were minimal (Fig. S8), indicating that the increased turbulent heat flux (up to approximately 32 W m$^{-2}$) was compensated by the

increased net radiation (up to approximately 52 W m$^{-2}$), suggesting that net shortwave radiation acted as the primary factor. Thus, LST increased as the residual heat increased (up to approximately 21 W m$^{-2}$).

**b. Croplands to grasslands**

In summer, the LST showed warming from croplands to grasslands (2.31 °C, Fig. S9). The net radiation decreased from croplands to grasslands (approximately -51 W m$^{-2}$ at daily maximum). The decreased turbulent energy fluxes (approximately -76 W m$^{-2}$ at daily maximum) into the atmosphere were decided by decreased latent heat fluxes (approximately -136 W m$^{-2}$ at daily maximum) rather than increased sensible heat fluxes (approximately 60 W m$^{-2}$ at daily maximum). Ultimately, the decreased net radiative energy input was compensated by the reduced turbulent heat fluxes during the day. Consequently, the results indicated that the LST increased during the day as the residual heat fluxes increased (approximately 25 W m$^{-2}$ at the daily maximum). At night, the reversed residual ground heat energy barely reduced the nocturnal LST because the energy increase at night was insufficient to compensate for the higher temperatures during the day (Breil et al., 2020).

In winter, the LST increased by 1.15 °C from croplands to grasslands. No significant differences were found between the bare land to grasslands and croplands to grasslands transitions, as croplands were considered to have no vegetation in winter after harvest.

## 3.2 Land use/cover composition

### 3.2.1 Effects of historical land use/cover composition

To explore the appropriate land use/cover composition, we analysed it from 2000 to 2015. For simplicity, we selected grid cells with a greater than 90 % composition of grasslands, bare land, and croplands. The ratio of the three main land types within each grid represents the land use/cover composition.

Fig. 4 illustrates the spatiotemporal heterogeneity of land use/cover composition. The impact of land use/cover composition change from 2000 to 2015 was assessed by comparing the differences between CN2015 and EXP2000 (Table S3). The results showed that grids transitioning from bare land to grasslands led to cooling and decreased WC, whereas grids transitioning from croplands to grasslands led to warming and increased WC, which is consistent with Section 3.1.2. However, the results also highlight that grids involving both bare land and croplands transitioning to grasslands led to increased warming and drying. This combination of LUCC impacts resulted in unclear or mixed spatially averaged effects. Therefore, the land use/cover composition for optimal ecosystem services is further explored in the next section.
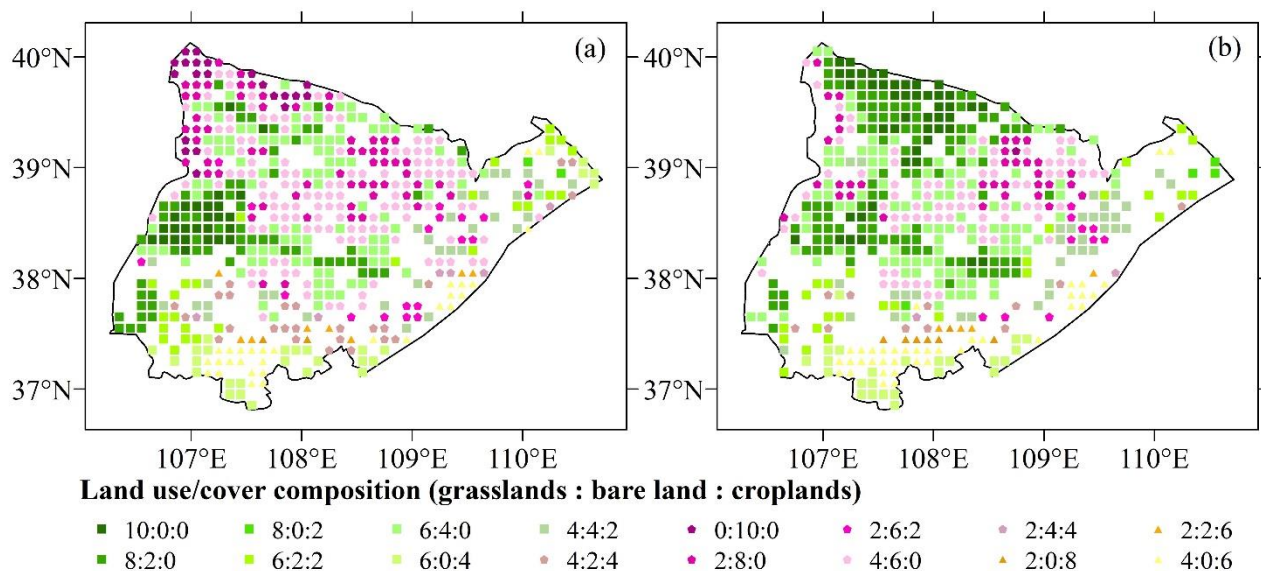
**Figure 4. The land use/cover composition in 0.1 ° grids of the study area in 2000 (a) and 2015 (b).**

### 3.2.2 Implication for future land use/cover composition

285 The government has proposed a plan to increase grassland coverage to 60 % by transforming bare land and croplands into grasslands (China state council, 2017; National development and reform commission, 2019). To assess the implications of this plan, we simulated future land use/cover scenarios with 60 % grassland, varying the proportions of bare land and croplands. These experiments assumed that land use conversions occurred exclusively among barren land (29.9 %), croplands (12.5 %), and grasslands (52.0 %), whereas other land use/cover classes (5.6 %), including shrublands, urban areas, water bodies, and

290 forests, remained constant and were excluded from the transformation process. Two extreme scenarios were defined: in EXP_603004, additional grassland was converted entirely from croplands, resulting in a land use/cover composition of 60 % grassland, 30 % bare land, and 4 % croplands; in EXP_602113, grassland expansion occurred through the conversion of bare land, resulting in a composition of 60 % grasslands, 21 % bare land, and 13 % croplands. Additionally, three intermediate scenarios were designed with incremental variations in the proportions of bare land and croplands: 60 %, 23 %, and 11 % for

295 EXP_602311; 60 %, 25 %, and 9 % for EXP_602509; 60 %, 27 %, and 7 % for EXP_602707.

The simulations of future land use/cover scenarios, compared with 2015 are presented in Table 2. Grassland expansion through the conversion of croplands (EXP_603004) resulted in significant variations in LST (0.09 °C) and ET (-17.62 mm yr$^{-1}$). nae. However, none of the scenarios had a significant negative impact on WC, indicating that the vegetation restoration efforts are unlikely to exacerbate drying. These findings suggest that increasing grassland coverage to 60% by 2035 maintains

300 ecohydrological stability while advancing vegetation restoration goals.

**Table 2. Spatially weighted averaged differences between future vegetation restoration scenarios and that in the year 2015.**

| | Δ LST (°C) | Δ ET (mm yr$^{-1}$) | Δ WC (mm yr$^{-1}$) |
| --- | --- | --- | --- |

| | | | |
|---|---|---|---|
| EXP_602113 | -0.04 | 4.14 | -5.71 |
| EXP_602311 | -0.01 | 0.70 | -0.44 |
| EXP_602509 | 0.02 | -5.50 | 4.79 |
| EXP_602707 | 0.05 | -10.34*** | 10.05 |
| EXP_603004 | 0.09* | -17.62*** | 17.98 |

Note: Statistical significance is denoted as follows: * indicates $p < 0.1$, ** indicates $p < 0.05$, *** indicates $p < 0.01$

## 4 Discussion

### 4.1 Sensitivity of LAI + SAI and vegetation height

305 In CLM5.0, a dual-source land surface model, the canopy-stored energy was assumed to be zero and massless. The vegetation vapour pressure, temperature, and latent heat fluxes were calculated iteratively using the Newton-Raphson method. This process is highly complex and involves several land surface parameters including surface albedo, roughness, LAI + SAI, aerodynamic resistance, vegetation height, and leaf stomatal resistance (Lawrence et al., 2019). As shown in Fig. S10, the Yanchi_height and Yanchi_laisai run behaved more like a Yanchi_grass simulation. LAI + SAI and vegetation height

310 influenced the surface roughness and aerodynamic resistance. These findings suggest that the interplay between complex processes cannot be simplified to adjustments in a single factor because other characteristics play indispensable roles. Future research on water and energy processes should focus on understanding the distribution of flux cycles, as discussed in Section 3.1.2.

### 4.2 Uncertainty of soil properties

315 In this study, the soil property dataset used for land surface modelling over China provided better precision than the default values in CLM5.0 (Fig. S11). However, uncertainties remain regarding soil input datasets. For example, the dataset indicates that sand content is less than 60 % and clay content is greater than 10 % in the northwest, which does not align with the characteristics of desertified areas (Duan et al., 2021; Liu et al., 2011; Xu, 2019). Additionally, experimental data from in-situ stations (Table S4) showed a higher sand content and lower clay content compared to the dataset. This discrepancy suggests

320 that the dataset does not accurately represent the realistic conditions of the region. Furthermore, the LUCC can result in significant changes in soil properties, particularly soil organic matter, sand, and clay content (Celik, 2005; Su et al., 2021). Dynamic changes in soil properties associated with LUCC were not considered in the model. To enhance the accuracy of future studies, it is necessary to incorporate a dynamic soil parameter model that accounts for the changes in soil properties caused by LUCC.

### 4.3 Limitations of the study

325

Ecohydrological sustainability focuses on the interaction between water and ecological systems, emphasizing water as a key driver (Zalewski, 2021). It includes: water provision, soil erosion, and biodiversity. (1) Water provision: WC is defined as the difference between water input and output, representing an ecosystem's capacity to store or retain water. Consequently, WC

reflects the amount of water that can be supplied to the region's interior (Bai et al., 2019; Costanza et al., 1997). (2) Soil erosion:

330     Severe soil erosion leads to widespread topsoil loss and conversion of the once-flat plateau into hills and gullies, leading to catastrophic floods and droughts in the Loess Plateau of China (Chen et al., 2007; Fu et al., 2017). Since the 1980s, vegetation restoration has converted sloping farmlands (>15 °) into forests and grasslands, resulting in a soil-retention rate of 84.4 % on slopes of 8 °–35 ° (Fu et al., 2017). However, in most APENWC areas, soil erosion rates were between 0–200 t km$^{-2}$ yr$^{-1}$ in 2000 and 2008 (Fu et al., 2011), and no significant changes were observed during the Grain-for-Green Project (Fu et al., 2017).

335     This stability is attributed to the APENWC's lack of intense gully-hilly areas, where severe soil erosion typically occurs. Therefore, the impact of soil erosion caused by vegetation restoration on the ecohydrological sustainability of the APENWC is limited. (3) Biodiversity: During vegetation restoration, the diversity of soil fauna and fungal communities increases because of the proliferation of fast-growing plant species that produce abundant litter and root exudates. These processes enhance the soil food web and promote nutrient cycling (Wu et al., 2021; Yang et al., 2021b). Soil water content between 20 and 60 cm

340     depths, along with soil properties, primarily explains variations in plant and soil fungal diversity, regardless of land use/cover class (Yang et al., 2017; Wang et al., 2021a). As soil water content is already captured by water conservation (WC), WC serves as the key factor influencing ecohydrological sustainability. Deng (2022) identified WC as a priority for improvement in the APENWC based on ecological sustainability assessments of vegetation restoration. Therefore, enhancing ecohydrological sustainability in the study area should focus primarily on improving WC.

345     In this study, we focused exclusively on LUCC impacts and designed experiments with varying land use/cover scenarios to assess future vegetation restoration. This approach has been widely adopted to isolate the LUCC effects (Wang et al., 2021b; Breil et al., 2020). However, water and energy processes are influenced by both the LUCC and climate, and vegetation-climate coupling remains a complex process. Future studies should examine the contributions of background climatic conditions.

## 5    Conclusions

350     This study utilised CLM5.0, validated with in-situ observations, to simulate and quantify the effects of historical LUCC in the APENWC. Five LUCC scenarios were also designed to assess the potential impacts of future LUCC in the region. The key findings are as follows: Firstly, the conversion of bare land to grasslands reduced LST, whereas the conversion of croplands to grasslands led to an increase in LST. The transition from bare land to grasslands increased ET, while the shift from croplands to grasslands decreased ET. Despite generating significant local effects, the overall effect of historical LUCC resulted in

355     negligible variations in LST and ET across the APENWC region. Further analysis of the different land use/cover compositional changes revealed that the combination of LUCC impacts led to unclear synergistic effects from vegetation restoration. Finally, simulations of future land use/cover scenarios with 60 % grassland cover and varying proportions of bare land and cropland indicated that grassland expansion through cropland conversions would slightly increase ET. However, none of the scenarios showed significant adverse effects on WC, suggesting that vegetation restoration will not exacerbate drying conditions.

## Data availability

The data will be made available on request

## Authorship contribution

Yuzuo Zhu: Conceptualization, Methodology, Software, Validation, Formal analysis, Writing - original draft.

Xuefeng Xu: Data curation, Writing - Review & Editing.

## Competing interest

We declare no competing interest.

## Acknowledgments

The study was supported by the National Natural Science Foundation of China (grant number: 42030501, 41530752 and 91125010). We thank Prof. Xin Jia and his team at Beijing Forestry University for sharing their in-situ ET observation data from 2015 at Yanchi Station to calibrate the performance of the CLM5.0 in this work.

## Reference

Alkama, R. and Cescatti, A.: Biophysical climate impacts of recent changes in global forest cover, Science, 351, 600-604, https://doi.org/10.1126/science.aac8083, 2016.

Arora, V. K. and Montenegro, A.: Small temperature benefits provided by realistic afforestation efforts, Nature Geoscience, 4, 514-518, https://doi.org/10.1038/ngeo1182, 2011.

Bai, Y., Ochuodho, T. O., and Yang, J.: Impact of land use and climate change on water-related ecosystem services in Kentucky, USA, Ecological Indicators, 102, 51-64, https://doi.org/10.1016/j.ecolind.2019.01.079, 2019.

Bonan, G. B., Oleson, K. W., Vertenstein, M., Levis, S., Zeng, X., Dai, Y., Dickinson, R. E., and Yang, Z.-L.: The Land Surface Climatology of the Community Land Model Coupled to the NCAR Community Climate Model*, Journal of Climate, 15, 3123-3149, https://doi.org/10.1175/1520-0442(2002)015<3123:Tlscot>2.0.Co;2, 2002.

Breil, M., Rechid, D., Davin, E. L., de Noblet-Ducoudré, N., Katragkou, E., Cardoso, R. M., Hoffmann, P., Jach, L. L., Soares, P. M. M., Sofiadis, G., Strada, S., Strandberg, G., Tölle, M. H., and Warrach-Sagi, K.: The Opposing Effects of Reforestation and Afforestation on the Diurnal Temperature Cycle at the Surface and in the Lowest Atmospheric Model Level in the European Summer, Journal of Climate, 33, 9159-9179, https://doi.org/10.1175/jcli-d-19-0624.1, 2020.

Burakowski, E., Tawfik, A., Ouimette, A., Lepine, L., Novick, K., Ollinger, S., Zarzycki, C., and Bonan, G.: The role of surface roughness, albedo, and Bowen ratio on ecosystem energy balance in the Eastern United States, Agricultural and Forest Meteorology, 249, 367-376, https://doi.org/10.1016/j.agrformet.2017.11.030, 2018.

Cai, X., Yang, Z.-L., David, C. H., Niu, G.-Y., and Rodell, M.: Hydrological evaluation of the Noah-MP land surface model for the Mississippi River Basin, Journal of Geophysical Research: Atmospheres, 119, 23-38, https://doi.org/10.1002/2013jd020792, 2014.

Cao, Q., Yu, D., Georgescu, M., Han, Z., and Wu, J.: Impacts of land use and land cover change on regional climate: a case study in the agro-pastoral transitional zone of China, Environmental Research Letters, 10, 124025, https://doi.org/10.1088/1748-9326/10/12/124025, 2015.

Celik, I.: Land-use effects on organic matter and physical properties of soil in a southern Mediterranean highland of Turkey, Soil and Tillage Research, 83, 270-277, https://doi.org/10.1016/j.still.2004.08.001, 2005.

Chen, L. and Dirmeyer, P. A.: Adapting observationally based metrics of biogeophysical feedbacks from land cover/land use change to climate modeling, Environmental Research Letters, 11, 034002, https://doi.org/10.1088/1748-9326/11/3/034002, 2016.

Chen, L. and Dirmeyer, P. A.: Global observed and modelled impacts of irrigation on surface temperature, International Journal of Climatology, 39, 2587-2600, https://doi.org/10.1002/joc.5973, 2018.

Chen, L. and Dirmeyer, P. A.: Differing Responses of the Diurnal Cycle of Land Surface and Air Temperatures to Deforestation, Journal of Climate, 32, 7067-7079, https://doi.org/10.1175/jcli-d-19-0002.1, 2019.

Chen, L., Wei, W., Fu, B., and Lü, Y.: Soil and water conservation on the Loess Plateau in China: review and perspective, Progress in Physical Geography: Earth and Environment, 31, 389-403, https://doi.org/10.1177/0309133307081290, 2007.

Cherubini, F., Huang, B., Hu, X., Tölle, M. H., and Strømman, A. H.: Quantifying the climate response to extreme land cover changes in Europe with a regional model, Environmental Research Letters, 13, 074002, https://doi.org/10.1088/1748-9326/aac794, 2018.

Notice of the state council on printing and distributing the outline of the national land plan (2016-2035): http://www.gov.cn/zhengce/content/2017-02/04/content_5165309.htm, last access: 2024.

Costanza, R., d'Arge, R., de Groot, R., Farberk, S., Grasso, M., Hannon, B., Limburg, K., Naeem, S., V. O'Neill, R., Paruelo, J., G. Raskin, R., Suttonkk, P., and van den Belt, M.: The value of the world's ecosystem services and natural capital, Nature, 387, 253-259, https://doi.org/10.1038/387253a0, 1997.

Das, P., Behera, M. D., Patidar, N., Sahoo, B., Tripathi, P., Behera, P. R., Srivastava, S. K., Roy, P. S., Thakur, P., Agrawal, S. P., and Krishnamurthy, Y. V. N.: Impact of LULC change on the runoff, base flow and evapotranspiration dynamics in eastern Indian river basins during 1985–2005 using variable infiltration capacity approach, Journal of Earth System Science, 127, https://doi.org/10.1007/s12040-018-0921-8, 2018.

Davin, E. L. and de Noblet-Ducoudré, D. N.: Climatic Impact of Global-Scale Deforestation: Radiative versus Nonradiative Processes, Journal of Climate, 23, 97-112, https://doi.org/10.1175/2009jcli3102.1, 2010.

Davin, E. L., Seneviratne, S. I., Ciais, P., Olioso, A., and Wang, T.: Preferential cooling of hot extremes from cropland albedo management, Proc Natl Acad Sci U S A, 111, 9757-9761, https://doi.org/10.1073/pnas.1317323111, 2014.

Davin, E. L., Rechid, D., Breil, M., Cardoso, R. M., Coppola, E., Hoffmann, P., Jach, L. L., Katragkou, E., de Noblet-Ducoudré, N., Radtke, K., Raffa, M., Soares, P. M. M., Sofiadis, G., Strada, S., Strandberg, G., Tölle, M. H., Warrach-Sagi, K., and Wulfmeyer, V.: Biogeophysical impacts of forestation in Europe: first results from the LUCAS (Land Use and Climate Across Scales) regional climate model intercomparison, Earth System Dynamics, 11, 183-200, https://doi.org/10.5194/esd-11-183-2020, 2020.

Deng: Research on ecological performance evaluation of the Sloping Land Conversion Program in the Loess Plateau (in Chinese), Ph.D thesis, Northwest A&F University, 131 pp., 2022.

Deng, M., Meng, X., Lyv, Y., Zhao, L., Li, Z., Hu, Z., and Jing, H.: Comparison of Soil Water and Heat Transfer Modeling Over the Tibetan Plateau Using Two Community Land Surface Model (CLM) Versions, Journal of Advances in Modeling Earth Systems, 12, 1942-2466, https://doi.org/10.1029/2020ms002189, 2020.

Ding, X., Zheng, M., and Zheng, X.: The Application of Genetic Algorithm in Land Use Optimization Research: A Review, Land, 10, https://doi.org/10.3390/land10050526, 2021.

Du, T., Jiao, J., Duan, H., He, H., XUE, X., and Xie, Y.: Study of conversion between landuse/landcover classification system of Chinese Academy of Science and IGBP classification system: In the northwest argo-pastoral zone Journal of Lanzhou University: Natural Science (in Chinese), 56, 91-95, https://doi.org/10.13885/j.issn.0455-2059.20120.01.011, 2020.

Duan, H., Xie, Y., Du, T., and Wang, X.: Random and systematic change analysis in land use change at the category level-A case study on Mu Us area of China, Sci Total Environ, 777, 145920, https://doi.org/10.1016/j.scitotenv.2021.145920, 2021.

Duveiller, G., Hooker, J., and Cescatti, A.: The mark of vegetation change on Earth's surface energy balance, Nat Commun, 9, 679, https://doi.org/10.1038/s41467-017-02810-8, 2018.

440 Findell, K. L., Berg, A., Gentine, P., Krasting, J. P., Lintner, B. R., Malyshev, S., Santanello, J. A., Jr., and Shevliakova, E.: The impact of anthropogenic land use and land cover change on regional climate extremes, Nat Commun, 8, 989, https://doi.org/10.1038/s41467-017-01038-w, 2017.

Fu, B., Liu, Y., Lü, Y., He, C., Zeng, Y., and Wu, B.: Assessing the soil erosion control service of ecosystems change in the Loess Plateau of China, Ecological Complexity, 8, 284-293, https://doi.org/10.1016/j.ecocom.2011.07.003, 2011.

445 Fu, B., Wang, S., Liu, Y., Liu, J., Liang, W., and Miao, C.: Hydrogeomorphic Ecosystem Responses to Natural and Anthropogenic Changes in the Loess Plateau of China, Annual Review of Earth and Planetary Sciences, 45, 223-243, https://doi.org/10.1146/annurev-earth-063016-020552, 2017.

Guo, X., Yao, Y., Zhang, Y., Lin, Y., Jiang, B., Jia, K., Zhang, X., Xie, X., Zhang, L., Shang, K., Yang, J., and Bei, X.: Discrepancies in the Simulated Global Terrestrial Latent Heat Flux from GLASS and MERRA-2 Surface Net Radiation

450 Products, Remote Sensing, 12, 2763, https://doi.org/10.3390/rs12172763, 2020.

Han, Y., Ma, Z., Li, M., and Chen, L.: Numerical simulation of the impact of land use/cover change on land surface process in China from 2001 to 2010, Climatic and Environmental Research (in Chinese), 26, 75-90, https://doi.org/10.3878/j.issn.1006-9585.2020.20039, 2021.

He, Y., Lee, E., and Mankin, J. S.: Seasonal tropospheric cooling in Northeast China associated with cropland expansion,

455 Environmental Research Letters, 15, 034032, https://doi.org/10.1088/1748-9326/ab6616, 2020.

Jia, X., Shao, M., Zhu, Y., and Luo, Y.: Soil moisture decline due to afforestation across the Loess Plateau, China, Journal of Hydrology, 546, 113-122, https://doi.org/10.1016/j.jhydrol.2017.01.011, 2017a.

Jia, X., Wang, Y., Shao, M., Luo, Y., and Zhang, C.: Estimating regional losses of soil water due to the conversion of agricultural land to forest in China's Loess Plateau, Ecohydrology, 10, e1851, https://doi.org/10.1002/eco.1851, 2017b.

460 Kaim, A., Cord, A. F., and Volk, M.: A review of multi-criteria optimization techniques for agricultural land use allocation, Environmental Modelling & Software, 105, 79-93, https://doi.org/10.1016/j.envsoft.2018.03.031, 2018.

Kucsicsa, G., Popovici, E.-A., Bălteanu, D., Grigorescu, I., Dumitrașcu, M., and Mitrică, B.: Future land use/cover changes in Romania: regional simulations based on CLUE-S model and CORINE land cover database, Landscape and Ecological Engineering, 15, 75-90, https://doi.org/10.1007/s11355-018-0362-1, 2019.

465 Kueppers, L. M. and Snyder, M. A.: Influence of irrigated agriculture on diurnal surface energy and water fluxes, surface climate, and atmospheric circulation in California, Climate Dynamics, 38, 1017-1029, https://doi.org/10.1007/s00382-011-1123-0, 2011.

Lawrence, D. M., Fisher, R. A., Koven, C. D., Oleson, K. W., Swenson, S. C., Bonan, G., Collier, N., Ghimire, B., Kampenhout, L., Kennedy, D., Kluzek, E., Lawrence, P. J., Li, F., Li, H., Lombardozzi, D., Riley, W. J., Sacks, W. J., Shi, M., Vertenstein,

470 M., Wieder, W. R., Xu, C., Ali, A. A., Badger, A. M., Bisht, G., Broeke, M., Brunke, M. A., Burns, S. P., Buzan, J., Clark, M., Craig, A., Dahlin, K., Drewniak, B., Fisher, J. B., Flanner, M., Fox, A. M., Gentine, P., Hoffman, F., Keppel-Aleks, G., Knox, R., Kumar, S., Lenaerts, J., Leung, L. R., Lipscomb, W. H., Lu, Y., Pandey, A., Pelletier, J. D., Perket, J., Randerson, J. T., Ricciuto, D. M., Sanderson, B. M., Slater, A., Subin, Z. M., Tang, J., Thomas, R. Q., Val Martin, M., and Zeng, X.: The Community Land Model Version 5: Description of New Features, Benchmarking, and Impact of Forcing Uncertainty, Journal

475 of Advances in Modeling Earth Systems, 11, 4245-4287, https://doi.org/10.1029/2018ms001583, 2019.

Lee, X., Goulden, M. L., Hollinger, D. Y., Barr, A., Black, T. A., Bohrer, G., Bracho, R., Drake, B., Goldstein, A., Gu, L., Katul, G., Kolb, T., Law, B. E., Margolis, H., Meyers, T., Monson, R., Munger, W., Oren, R., Paw, U. K., Richardson, A. D., Schmid, H. P., Staebler, R., Wofsy, S., and Zhao, L.: Observed increase in local cooling effect of deforestation at higher latitudes, Nature, 479, 384-387, https://doi.org/10.1038/nature10588, 2011.

480 Li, F.: Assessment and fusion of the soil moisture data sets based on community land model and smap satellite (in Chinese), M.S. thesis, Lanzhou Univeristy, 16-40 pp., 2021.

Li, G., Zhang, F., Jing, Y., Liu, Y., and Sun, G.: Response of evapotranspiration to changes in land use and land cover and climate in China during 2001-2013, Sci Total Environ, 596-597, 256-265, https://doi.org/10.1016/j.scitotenv.2017.04.080, 2017.

485 Li, X., Yang, L., Tian, W., Xu, X., and He, C.: Land use and land cover change in agro-pastoral ecotone in Northern China: A review, Chinese Journal of Applied Ecology (in Chinese), 29, 3487-3495, https://doi.org/10.13287/j.1001-9332.201810.020, 2018.

Li, X., Xu, X., Wang, X., Xu, S., Tian, W., Tian, J., and He, C.: Assessing the Effects of Spatial Scales on Regional Evapotranspiration Estimation by the SEBAL Model and Multiple Satellite Datasets: A Case Study in the Agro-Pastoral Ecotone, Northwestern China, Remote Sensing, 13, 1524, https://doi.org/10.3390/rs13081524, 2021.

Li, Y., Zhao, M., Motesharrei, S., Mu, Q., Kalnay, E., and Li, S.: Local cooling and warming effects of forests based on satellite observations, Nat Commun, 6, 6603, https://doi.org/10.1038/ncomms7603, 2015.

Liang, W., Bai, D., Wang, F., Fu, B., Yan, J., Wang, S., Yang, Y., Long, D., and Feng, M.: Quantifying the impacts of climate change and ecological restoration on streamflow changes based on a Budyko hydrological model in China's Loess Plateau, Water Resources Research, 51, 6500-6519, https://doi.org/10.1002/2014wr016589, 2015.

Liu, J., Shao, Q., Yan, X., Fan, J., Zhan, J., Deng, X., Kuang, W., and Huang, L.: The climatic impacts of land use and land cover change compared among countries, Journal of Geographical Sciences, 26, 889-903, https://doi.org/10.1007/s11442-016-1305-0, 2016.

Liu, P., Zha, T., Jia, X., Black, T. A., Jassal, R. S., Ma, J., Bai, Y., and Wu, Y.: Different Effects of Spring and Summer Droughts on Ecosystem Carbon and Water Exchanges in a Semiarid Shrubland Ecosystem in Northwest China, Ecosystems, 22, 1869-1885, https://doi.org/10.1007/s10021-019-00379-5, 2019.

Liu, Y., Li, J., and Bao, Y.: Dynamic analysis of desertification in the western of Ordos Plateau-The case of Etoke Banner, Journal of Inner Mongolia Agricultural University (In Chinese), 32, 81-87, https://doi.org/CNKI:SUN:NMGM.0.2011-04-017, 2011.

Llopart, M., Reboita, M., Coppola, E., Giorgi, F., da Rocha, R., and de Souza, D.: Land Use Change over the Amazon Forest and Its Impact on the Local Climate, Water, 10, 149, https://doi.org/10.3390/w10020149, 2018.

Luo, Q., Wen, J., Hu, Z., Lu, Y., and Yang, X.: Parameter Sensitivities of the Community Land Model at Two Alpine Sites in the Three-River Source Region, Journal of Meteorological Research, 34, 851-864, https://doi.org/10.1007/s13351-020-9205-8, 2020.

Ma, X., Jin, J., Zhu, L., and Liu, J.: Evaluating and improving simulations of diurnal variation in land surface temperature with the Community Land Model for the Tibetan Plateau, PeerJ, 9, e11040, https://doi.org/10.7717/peerj.11040, 2021.

Meier, R., Davin, E. L., Lejeune, Q., Hauser, M., Li, Y., Martens, B., Schultz, N. M., Sterling, S., and Thiery, W.: Evaluating and improving the Community Land Model's sensitivity to land cover, Biogeosciences, 15, 4731-4757, https://doi.org/10.5194/bg-15-4731-2018, 2018.

Major projects for ecological protection and restoration support systems: http://gi.mnr.gov.cn/202006/t20200611_2525741.html, last access: 2024.

Ning, J., Gao, Z., and Xu, F.: Effects of land cover change on evapotranspiration in the Yellow River Delta analyzed with the SEBAL model, Journal of Applied Remote Sensing, 11, 016009, https://doi.org/10.1117/1.Jrs.11.016009, 2017.

Nkhoma, L., Ngongondo, C., Dulanya, Z., and Monjerezi, M.: Evaluation of integrated impacts of climate and land use change on the river flow regime in Wamkurumadzi River, Shire Basin in Malawi, Journal of Water and Climate Change, 12, 1674-1693, https://doi.org/10.2166/wcc.2020.138, 2021.

Poniatowski, D., Beckmann, C., Löffler, F., Münsch, T., Helbing, F., Samways, M. J., Fartmann, T., and Lancaster, L.: Relative impacts of land-use and climate change on grasshopper range shifts have changed over time, Global Ecology and Biogeography, 29, 2190-2202, https://doi.org/10.1111/geb.13188, 2020.

Shangguan, W. and Dai, Y.: A China Dataset of soil hydraulic parameters pedotransfer functions for land surface modeling (1980), National Tibetan Plateau/Third Pole Environment Data Center [data set], https://doi.org/10.11888/Soil.tpdc.270281, 2013.

Srivastava, P. K., Han, D., Islam, T., Petropoulos, G. P., Gupta, M., and Dai, Q.: Seasonal evaluation of evapotranspiration fluxes from MODIS satellite and mesoscale model downscaled global reanalysis datasets, Theoretical and Applied Climatology, 124, 461-473, https://doi.org/10.1007/s00704-015-1430-1, 2015.

Su, Y., Zhang, Y., Shang, L., Wang, S., Hu, G., Song, M., and Zhou, K.: Root-induced alterations in soil hydrothermal properties in alpine meadows of the Qinghai-Tibet Plateau, Rhizosphere, 20, 2176, https://doi.org/10.1016/j.rhisph.2021.100451, 2021.

Tan, X., Zhang, L., He, C., Zhu, Y., Han, Z., and Li, X.: Applicability of cosmic-ray neutron sensor for measuring soil moisture at the agricultural-pastoral ecotone in northwest China, Science China Earth Sciences, 63, 1730-1744, https://doi.org/10.1007/s11430-020-9650-2, 2020.

Tölle, M. H., Breil, M., Radtke, K., and Panitz, H.-J.: Sensitivity of European Temperature to Albedo Parameterization in the Regional Climate Model COSMO-CLM Linked to Extreme Land Use Changes, Frontiers in Environmental Science, 6, 123, https://doi.org/10.3389/fenvs.2018.00123, 2018.

540 Wan, Z., Hook, S., and Hulley, G.: MOD11C1 (6), NASA [data set], https://doi.org/10.5067/MODIS/MOD11C1.006, 2015.

Wang, H., Xiao, W., Zhao, Y., Wang, Y., Hou, B., Zhou, Y., Yang, H., Zhang, X., and Cui, H.: The Spatiotemporal Variability of Evapotranspiration and Its Response to Climate Change and Land Use/Land Cover Change in the Three Gorges Reservoir, Water, 11, 1739, https://doi.org/10.3390/w11091739, 2019a.

Wang, L., Wang, X., Chen, L., Song, N. P., and Yang, X. G.: Trade-off between soil moisture and species diversity in semi-
545 arid steppes in the Loess Plateau of China, Sci Total Environ, 750, 141646, https://doi.org/10.1016/j.scitotenv.2020.141646, 2021a.

Wang, W., Sun, L., and Luo, Y.: Changes in Vegetation Greenness in the Upper and Middle Reaches of the Yellow River Basin over 2000–2015, Sustainability, 11, 2176, https://doi.org/10.3390/su11072176, 2019b.

Wang, X., Zhang, B., Xu, X., Tian, J., and He, C.: Regional water-energy cycle response to land use/cover change in the agro-
550 pastoral ecotone, Northwest China, Journal of Hydrology, 580, 124246, https://doi.org/10.1016/j.jhydrol.2019.124246, 2020.

Wang, X., Zhang, B., Li, F., Li, X., Li, X., Wang, Y., Shao, R., Tian, J., and He, C.: Vegetation restoration projects intensify intraregional water recycling processes in the agro-pastoral ecotone of Northern China, Journal of Hydrometeorology, https://doi.org/10.1175/jhm-d-20-0125.1, 2021b.

Wang, Y., Ye, Z., Qiao, F., Li, Z., Miu, C., Di, Z., and Gong, W.: Review on connotation and estimation method of water
555 conservation, South-to-North Water Transfers and Water Science & Technology (in Chinese), 19, 1041-2017, https://doi.org/10.23476/j.cnki.nsbdqk.2021.0109, 2021c.

Wei, B., Xie, Y., Jia, X., Wang, X., He, H., and Xue, X.: Land use/land cover change and it's impacts on diurnal temperature range over the agricultural pastoral ecotone of Northern China, Land Degradation & Development, 29, 3009-3020, https://doi.org/10.1002/ldr.3052, 2018.

560 Winckler, J., Reick, C. H., and Pongratz, J.: Robust Identification of Local Biogeophysical Effects of Land-Cover Change in a Global Climate Model, Journal of Climate, 30, 1159-1176, https://doi.org/10.1175/jcli-d-16-0067.1, 2017.

Winckler, J., Reick, C. H., Luyssaert, S., Cescatti, A., Stoy, P. C., Lejeune, Q., Raddatz, T., Chlond, A., Heidkamp, M., and Pongratz, J.: Different response of surface temperature and air temperature to deforestation in climate models, Earth System Dynamics Discussions, 1-17, https://doi.org/10.5194/esd-2018-66, 2018.

565 Woodward, C., Shulmeister, J., Larsen, J., Jacobsen, G. E., and Zawadzki, A.: The hydrological legacy of deforestation on global wetlands, Science 346, 844-847, https://doi.org/10.1126/science.1260510, 2014.

Wu, Y., Chen, W., Entemake, W., Wang, J., Liu, H., Zhao, Z., Li, Y., Qiao, L., Yang, B., Liu, G., and Xue, S.: Long-term vegetation restoration promotes the stability of the soil micro-food web in the Loess Plateau in North-west China, Catena, 202, https://doi.org/10.1016/j.catena.2021.105293, 2021.

570 Wu, Z., Wu, J., Liu, J., He, B., Lei, T., and Wang, Q.: Increasing terrestrial vegetation activity of ecological restoration program in the Beijing–Tianjin Sand Source Region of China, Ecological Engineering, 52, 37-50, https://doi.org/10.1016/j.ecoleng.2012.12.040, 2013.

Xu, X.: Ningxia statistical yearbook, China Statistic Press, 381 pp., ISBN 978-7-5037-8514-6, 2018.

Xu, X., Li, X., Wang, X., He, C., Tian, W., Tian, J., and Yang, L.: Estimating daily evapotranspiration in the agricultural-
575 pastoral ecotone in Northwest China: A comparative analysis of the Complementary Relationship, WRF-CLM4.0, and WRF-Noah methods, Sci Total Environ, 729, 138635, https://doi.org/10.1016/j.scitotenv.2020.138635, 2020.

Xu, Z.: Study on ecological environment influencing factors and comprehensive evaluation of typical pastoral areas in western China (in Chinese), M.S. thesis, Xi'an University of Technology, 38-39 pp., 2019.

Xue, Y., Zhang, B., He, C., and Shao, R.: Detecting Vegetation Variations and Main Drivers over the Agropastoral Ecotone
580 of Northern China through the Ensemble Empirical Mode Decomposition Method, Remote Sensing, 11, 1860, https://doi.org/10.3390/rs11161860, 2019.

Yang, J.: Ordos statistical yearbook, China Statistics Press, 180 pp., ISBN 978-7-5037-8711-9, 2021.

Yang, K. and He, J.: China meteorological forcing dataset (1979-2018), National Tibetan Plateau/Third Pole Environment Data Center [data set], https://doi.org/10.11888/AtmosphericPhysics.tpe.249369.file, 2016.

585 Yang, L., Horion, S., He, C., and Fensholt, R.: Tracking Sustainable Restoration in Agro-Pastoral Ecotone of Northwest China, Remote Sensing, 13, 5031, https://doi.org/10.3390/rs13245031, 2021a.

Yang, L., Xie, Y., Zong, L., Qiu, T., and Jiao, J.: Land use optimization configuration based on multi- objective genetic algorithm and FLUS model of agro- pastoral ecotone in Northwest China, Journal of Geo-information Science (in Chinese), 22, 568-579, https://doi.org/10.12082/dqxxkx.2020.190531, 2020.

590    Yang, X., Shao, M. a., Li, T., Gan, M., and Chen, M.: Community characteristics and distribution patterns of soil fauna after vegetation restoration in the northern Loess Plateau, Ecological Indicators, 122, https://doi.org/10.1016/j.ecolind.2020.107236, 2021b.

Yang, Y., Dou, Y., Huang, Y., and An, S.: Links between Soil Fungal Diversity and Plant and Soil Properties on the Loess Plateau, Frontiers in Microbiology, 8, https://doi.org/10.3389/fmicb.2017.02198, 2017.

595    Yang, Z. L., Dickinson, R. E., Henderson-Sellers, A., and Pitman, A. J.: Preliminary study of spin-up processes in land surface models with the first stage data of Project for Intercomparison of Land Surface Parameterization Schemes Phase 1(a), Journal of Geophysical Research, 100, 16553-16578, https://doi.org/10.1029/95jd01076, 1995.

Yao, Y., Liang, S., Li, X., Hong, Y., Fisher, J. B., Zhang, N., Chen, J., Cheng, J., Zhao, S., Zhang, X., Jiang, B., Sun, L., Jia, K., Wang, K., Chen, Y., Mu, Q., and Feng, F.: Bayesian multimodel estimation of global terrestrial latent heat flux from eddy
600    covariance, meteorological, and satellite observations, Journal of Geophysical Research: Atmospheres, 119, 4521-4545, https://doi.org/10.1002/2013jd020864, 2014.

Zalewski, M.: Ecohydrology: An Integrative Sustainability Science, London, UK: IntechOpen, 53-61 pp., 2021.

Zeng, L. and Li, J.: A Bayesian belief network approach for mapping water conservation ecosystem service optimization region, Journal of Geographical Sciences, 29, 1021-1038, https://doi.org/10.1007/s11442-019-1642-x, 2019.

605    Zhang, K., Kimball, J. S., Nemani, R. R., and Running, S. W.: A continuous satellite-derived global record of land surface evapotranspiration from 1983 to 2006, Water Resources Research, 46, W09522, https://doi.org/10.1029/2009wr008800, 2010.

Zhang, L., He, C., Tian, W., and Zhu, Y.: Evaluation of Precipitation Datasets from TRMM Satellite and Down-scaled Reanalysis Products with Bias-correction in Middle Qilian Mountain, China, Chinese Geographical Science, 31, 474-490, https://doi.org/10.1007/s11769-021-1205-9, 2021.

610    Zhang, S., Yang, H., Yang, D., and Jayawardena, A. W.: Quantifying the effect of vegetation change on the regional water balance within the Budyko framework, Geophysical Research Letters, 43, 1140-1148, https://doi.org/10.1002/2015gl066952, 2016.

Zhang, S., Yang, D., Yang, Y., Piao, S., Yang, H., Lei, H., and Fu, B.: Excessive Afforestation and Soil Drying on China's Loess Plateau, Journal of Geophysical Research: Biogeosciences, 123, 923-935, https://doi.org/10.1002/2017jg004038, 2018.

615